Articles

Fluorination of Arc-Produced Carbon Material Containing Multiwall Nanotubes

Nicolai F. Yudanov, Alexander V. Okotrub, Yuri V. Shubin, Lyudmila I. Yudanova, and Lyubov G. Bulusheva*

Institute of Inorganic Chemistry SB RAS, av.Ak.Lavrentieva 3, 630090 Novosibirsk, Russian Federation

Andrew L. Chuvilin

Boreskov Institute of Catalysis SB RAS, av.Ak.Lavrentieva 5, 630090 Novosibirsk, Russian Federation

Jean-Marc Bonard

Institut de Physique Experimentale, Ecole Polytechnique Fédérale de Lausanne, CH-1015 Lausanne, Switzerland

Received April 9, 2001. Revised Manuscript Received February 12, 2002

The fluorination of arc-produced carbon material, which contained multiwall carbon nanotubes, was performed at room temperature by using a gaseous mixture of BrF_3 and Br_2. The elemental composition of the sample was determined by X-ray photoelectron spectroscopy to be $CF_{0.3}Br_{0.02}$, while graphite is fluorinated up to a C_2F stoichiometry under the same reaction conditions. The fluorinated carbon material and graphite fluoride were comparatively analyzed by means of X-ray diffraction, infrared spectroscopy, and thermogravimetry. Transmission electron microscopy indicated that only the outer shells of carbon nanotubes and polyhedral particles were fluorinated whereas the inner shells remained intact. We suggest that some of the arc-produced multiwall carbon nanotubes are composed of concentric cylindrical shells surrounded by nestled scrolls.

1. Introduction

The most important challenges of multiwall carbon nanotube (MWNT) chemistry are currently the synthesis of novel materials attractive for different applications and the determination of the tube structure. Fluorination of MWNTs is of special interest because the reactions of graphite with fluorine and various fluorinating agents have been well-studied.[1,2] As the structural properties of MWNTs are close to those of graphite, the synthesis techniques developed for graphite fluorination are expected to be applicable to nanotube-based materials. Furthermore, fluorination has been shown to possess a unique ability to control the chemical and physical properties of carbon materials.[3]

The reactivity of graphite and MWNTs, synthesized by the thermal decomposition of hydrocarbons on metal catalysts, with fluorine has been compared in ref 4. The nanotube samples were found to be completely fluorinated (C/F = 1) at lower temperatures than graphite. Using a gaseous mixture of F_2, HF, and IF_5, fluorinated nanotube compounds CF_x with $x \leq 0.4$ were produced at room temperature. Under the same conditions, the degree of fluorination (x) of graphite varied from 0.5 to 0.9 and the fluorides were introduced between the CF_x layers.[5] Open-ended MWNTs prepared by a template carbonization technique have been shown to react with fluorine even at 50 °C and covalent C−F bonds are formed on the internal surfaces of the tubes.[6] An investigation of the reactivity of single-wall carbon nanotubes in "bucky paper" form with elemental fluorine has revealed that there is a limiting stoichiometry of C_2F for which the fluorinated tube can still maintain its tubelike structure.[7] The high degree of solvation of fluorinated tubes in a variety of alcohol solvents could provide precursors for solid-state chemistry.[8]

(1) Watanabe, N.; Nakajima, T.; Touhara, H. In *Studies in Inorganic Chemistry, Vol.8. Graphite Fluorides*; Elsevier: Amsterdam, 1988.
(2) Hamwi, A. *J. Phys. Chem. Solids* **1996**, *57*, 677.
(3) Touhara, H.; Okino, F. *Carbon* **2000**, *38*, 241.
(4) Hamwi, A.; Alvergnat, H.; Bonnamy, S.; Beguin, F. *Carbon* **1997**, *35*, 723.
(5) Hamwi, A.; Daoud, M.; Cousseins, J. C. *Synth. Met.* **1989**, *30*, 23.
(6) Hattori, Y.; Watanabe, Y.; Kawasaki, S.; Okino, F.; Pradhan, B. K.; Kyotani, T.; Tomita, A.; Touhara, H. *Carbon* **1999**, *37*, 1033.
(7) Mickelson, E. T.; Huffman, C. B.; Rinzler, A. G.; Smalley, R. E.; Hauge, R. H.; Margrave, J. L. *Chem. Phys. Lett.* **1998**, *296*, 188.
(8) Mickelson, E. T.; Chiang, I. W.; Zimmerman, J. L.; Boul, P. J.; Lozano, J.; Liu, J.; Smalley, R. E.; Hauge, R. H.; Margrave, J. L. *J. Phys. Chem. B* **1999**, *103*, 4318.

10.1021/cm0103141 CCC: $22.00
Published on Web 03/21/2002

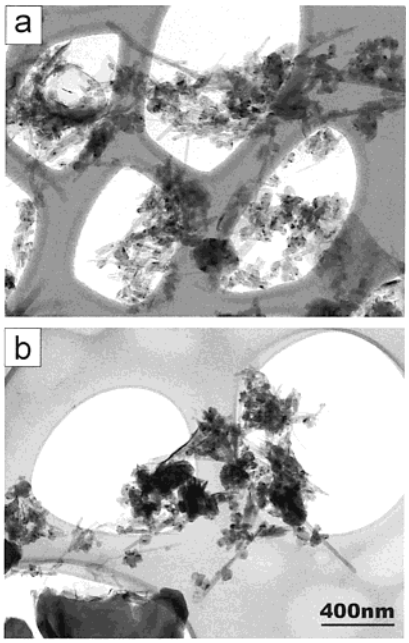

Figure 1. Low-magnification TEM micrograph of the (a) pristine and (b) fluorinated arc-produced carbon material.

In this work we studied the fluorination process of MWNTs produced in an electric arc. Unlike the nanotubes prepared by catalytic techniques, the arc-produced nanotubes are straight and well-graphitized with closed ends and with a smaller density of surface defects. A gaseous mixture of BrF_3 and Br_2 was used as the fluorinating agent because of its ability to fluorinate graphite at room temperature.[9] Possible structural models of the MWNTs are discussed based on electron microscopy images of particles found in the pristine and fluorinated carbon material.

2. Experimental Methods

Carbon material was synthesized by using a setup for arc-discharge graphite evaporation described elsewhere.[10] The diameter of the lower graphite cathode was 60 mm. The upper movable anode was combined from seven 6-mm-diameter and 200-mm-length graphite rods commonly used for spectrometric analysis. The anode was evaporated in a helium atmosphere and a dc arc current of 1000 A at 35−40 V for ≈15−20 min. Under these synthesis conditions the content of carbon nanotubes in the inner part of the deposit grown onto the cathode has been found to be strongly dependent on the gas pressure in the reactor chamber.[11] A transmission electron microscopy (TEM) micrograph of a typical sample prepared in helium gas at 800 Torr is presented in Figure 1a. The micrograph shows the coexistence of different kinds of particles: nanotubes having lengths ranging from 40 to 400 nm, polyhedral and globular particles of 150−200 Å in diameter, and graphite flakes. The number of shells of tubular and polyhedral nanoparticles varied from 2 to 30. The diameter of the inner channel of the carbon nanotubes is 30−50 Å and the outer diameter is 100−150 Å.

Prior to fluorination, the samples cut from the carbon deposit were crushed into 3−4-mm-size pieces. A typical experiment was conducted as follows. The sample (0.5 g) was placed in a Teflon flask and held in the vapor over liquid Br_2 for 24 h and then in the vapor over a solution of BrF_3 (2 g) in Br_2 (5 g) for 7 days. Thereafter, the flask content was dried under a flow of N_2 until the termination of Br_2 evolution (≈48 h). Oxidation of graphite with the same procedure makes it possible to prepare graphite fluoride with a limiting composition of $C_2F_{1.02\pm0.01}$.

Characterization of the samples was performed by using transmission electron microscopy (JEM-2010 and Philips EM430 microscopes), X-ray diffraction (DRON-SEIFERT-RM4 instrument, Cu Kα radiation), infrared spectroscopy (Specord IR 75 spectrometer for KBr pellet), X-ray photoelectron spectroscopy (VG Microtech spectrometer with Mg Kα line), and thermogravimetry (MOM C-derivatograph).

Results and Discussion

3.1. Chemical Composition. The fluorinated carbon material has a black color in contrast to the fluorinated natural graphite C_2F and fullerene $C_{60}F_{24}$,[12] which are respectively brown and light yellow. The carbon content in the samples prepared in two independent experiments was determined by mass uptake to be equal to 51.0 and 49.6 wt %. The presence of three elements in the produced material was detected by X-ray photoelectron spectroscopy: carbon, fluorine, and bromine with a ratio of C/F/Br = 1/0.3/0.02, as measured from the areas of the C 1s, F 1s, and Br 3d peaks with allowance for the cross sections. The carbon content calculated for this composition is equal to 62.2 wt %, which is larger than that determined by weighing the sample. This discrepancy may be attributed to the elimination of a portion of intercalated bromine from the sample irradiated in the vacuum chamber of the X-ray spectrometer. Proof of the presence of Br_2 molecules in the fluorinated sample is the yellow color that developed when the sample was treated with liquid CH_3CN. The acetonitrile molecules are most likely to substitute for the bromine, as occurs in the treatment of the intercalation compounds $C_2F_x{\cdot}yBr_2$ ($x \leq 1$, $y \approx 0.13$) by liquid or gaseous CH_3CN.

3.2. Nature of the C−F Bond. Comparative analysis of the fluorinated carbon material and C_2F by means of X-ray photoelectron and infrared (IR) spectroscopy revealed a similar character of the C−F bonding in these compounds. The values of C 1s binding energies for the carbon atoms bonded to fluorine that were observed in both compounds coincide and are equal to 288.6 eV. The IR spectrum of the fluorinated carbon material shows three peaks at 1050, 1110, and 1240 cm^{-1}, which are also characteristic of C_2F.[13] The IR spectra of samples that were prepared by a low-temperature fluorination of catalytic MWNTs exhibited vibrations[4] similar to those in our spectrum.

3.3. Thermal Stability. The thermal stability of the fluorinated sample was examined by thermogravimetry (TG) and differential thermal analysis (DTA) in air and in a helium atmosphere. The heating rate was 20 °C/min. The sample was readily decomposed when heated in air, while in a helium atmosphere its weight was almost unchanged below 415 °C. The DTA exhibited an exothermic peak having considerably higher intensity

(9) Yudanov, N. F.; Chernyavskii, L. I.*Russ. J. Struct. Chem.* **1987**, *28*, 534 [English Translation].
(10) Okotrub, A. V.; Romanov, D. A.; Chuvilin, A. L.; Shevtsov, Yu. V.; Gutakovskii, A. K.; Bulusheva, L. G.; Mazalov, L. N.*Phys. Low.-Dimen. Struct.* **1995**, *8/9*, 139.
(11) Okotrub, A. V.; Bulusheva, L. G.; Romanenko, A. I.; Chuvilin, A. L.; Rudina, N. A.; Shubin, Yu. V.; Yudanov, N. F.; Gusel'nikov, A. V. *Appl. Phys. A* **2001**, *71*, 481.
(12) Yudanov, N. F.; Okotrub, A. V.; Bulusheva, L. G.; Asanov, I. P.; Lisoivan, V. I.; Shevtsov, Yu. V. *Mol. Mater.* **1996**, *7*, 127.
(13) Bulusheva, L. G.; Okotrub, A. V. *Rev. Inorg. Chem.* **1999**, *19*, 79.

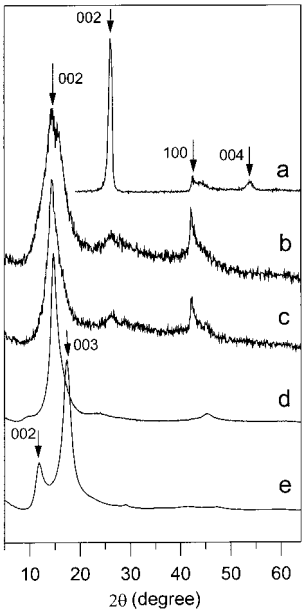

Figure 2. X-ray diffraction from (a) pristine and (b)−(d) fluorinated carbon material: (b) freshly fluorinated sample; (c) the same sample 4 months after preparation; (d) graphite fluoride C_2F; (e) C_2F intercalated by bromine to the composition $C_2F{\cdot}0.13Br_2$.

for the process occurring in air. In this experiment the decomposition was completed at 560 °C with a final weight loss of almost 60%, close to that of C_2F.[1] Decomposition of the fluorinated carbon material in a helium atmosphere ended at 590 °C with a 45% weight loss.

3.4. Structure and Morphology. Figure 1 compares low-magnification TEM micrographs obtained on the pristine and fluorinated carbon material. One can see that nanotubes and polyhedral nanoparticles are still present in the latter sample (Figure 1b).

The X-ray diffraction (XRD) patterns of the pristine carbon material and the fluorinated one are compared in Figure 2. The diffractogram of the former (Figure 2a) is typical for arc-produced multiwall carbon nanoparticles,[14,15] where the main peaks correspond to the 002, 100, and 004 reflections from the graphite lattice. The fluorination of the carbon material drastically changes the XRD pattern (Figure 2b,c). The position and asymmetric shape of the most intense line are quite similar to those of the 002 reflection in the XRD pattern of C_2F (Figure 2d). The line broadening may be caused by the lower stacking order of the layers in the fluorinated carbon material. The structure of the dominant line was revealed to vary with time. In particular, its width and the intensity of a shoulder at $2\theta = 15.7°$ (Figure 2b) are significantly reduced in the XRD pattern measured 4 months after preparation (Figure 2c). Again, these changes may be explained by the progressive removal and deintercalation of bromine from the sample, which contains particles having too small a size to produce a stable intercalate with bromine. Actually, C_2F forms a second stage intercalation compound with bromine. The XRD pattern of this intercalate, having a $C_2F{\cdot}0.13Br_2$ composition, is characterized by 002 ($2\theta = 11.9°$) and 003 ($2\theta = 17.4°$) reflections (Figure 2e), which are located respectively to the left and to the right sides of the 002 reflection of C_2F. The dominant peak of the freshly fluorinated sample could be broadened because of the reflections from the nanoparticle regions intercalated by bromine. The discrepancy between the positions of the 003 reflection of $C_2F{\cdot}0.13Br_2$ and the high-angle shoulder of the fresh sample reflects the lack of order between the intercalated layers in the nanoparticles.

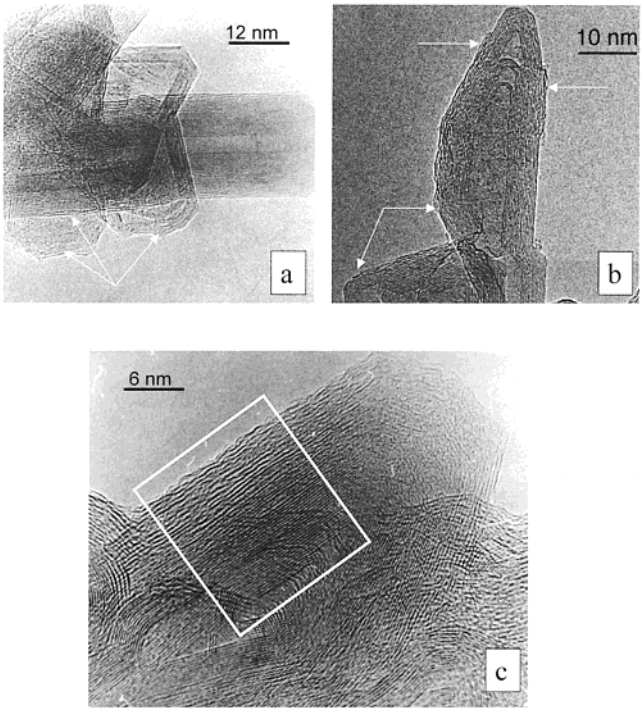

Figure 3. TEM micrographs of fluorinated multiwall carbon nanoparticles. The arrows show the sections with increased interlayer spacing as compared to that of graphite.

The XRD patterns of the fluorinated samples show the 002 and 100 reflections of the graphite lattice, which are missing from the C_2F pattern. Because the graphite sheets are certainly fluorinated under the synthesis conditions employed, these reflections can arise only from cylindrical or polyhedral concentric carbon layers preserved in the fluorinated sample. The enhanced intensity of the line at 42.5° with respect to that for the pristine sample is caused by the additional intensity contributed by the 200 reflection of the fluorinated carbon layers.

The XPS and XRD measurements on the fluorinated sample indicated that under the applied synthesis conditions the arc-produced nanoparticles did not undergo complete fluorination up to the C_2F composition, in contrast to the crystalline graphite. Retention of intact carbon tubular and polyhedral structures in the product was confirmed by high-resolution transmission electron microscopy (Figure 3). The HRTEM images indicate an increase in the interlayer spacing only between the outer shells following their fluorination, while the inner layers remained well-graphitized. While the surfaces of some particles are evenly fluorinated (Figure 3a), the partial destruction of the outer shells in another particles is observed (Figure 3b). The tube

(14) Zhou, O.; Fleming, R. M.; Murphy, D. W.; Chen, C. H.; Haddon, R. C.; Ramirez, A. P.; Glarum, S. H. *Science* **1994**, *263*, 1744.
(15) Mordkovich, V. Z.; Baxendale, M.; Yoshimura, S.; Chang, R. P. H. *Carbon* **1996**, *34*, 1301.

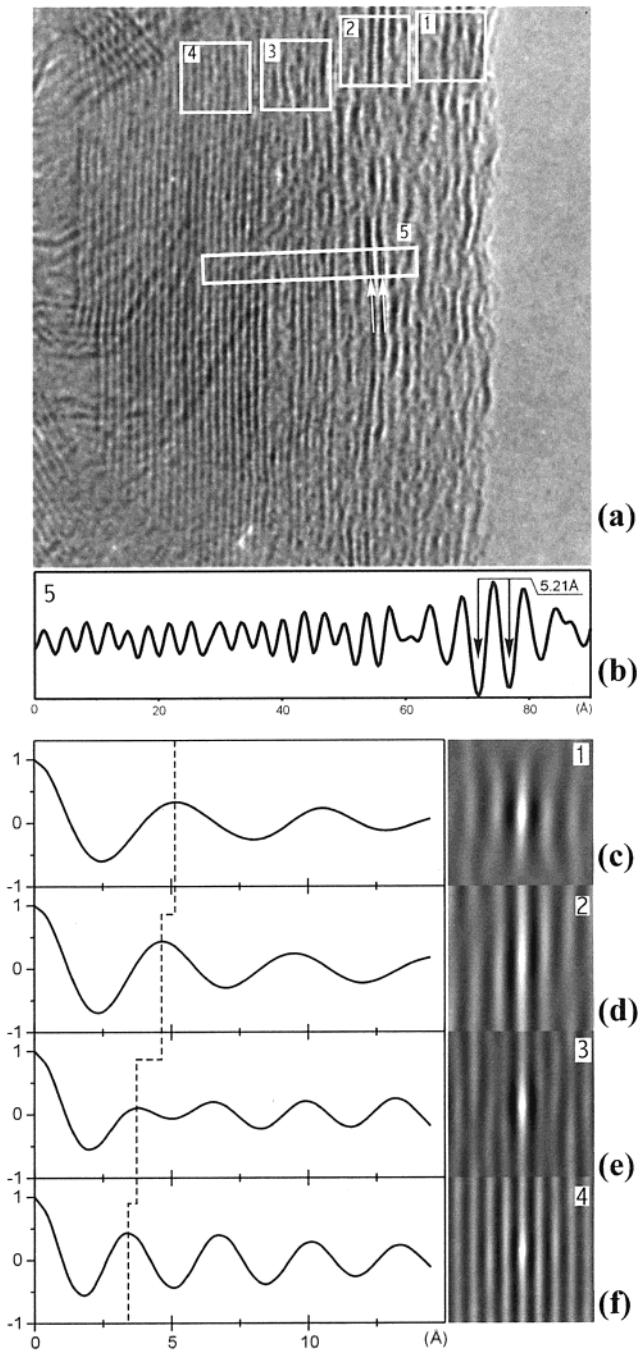

Figure 4. (a) Detail of the partially fluorinated tube taken from the TEM micrograph presented in Figure 3c with (b) a profile of the image intensity from region 5 and (c)−(f) the autocorrelation for the regions 1−4. The arrows show the fluorinated layers whose spacing estimated from the intensity profile is 5.21 Å. The dashed vertical lines indicate the average interlayer distance within regions 1−4.

tops are on occasion more fluorinated than the tube walls (Figure 3c), which may be due to the higher concentration of defects.

The micrograph in Figure 4a represents an enlarged fragment of the tube wall of Figure 3c, with four small regions, 1−4, selected along the tube diameter and a fifth region, 5, covering a larger distance. A profile of the image intensity (Figure 4b) was obtained from the region 5. The maxima and minima correspond to bright and dark image lines, which were initially averaged over the region width to suppress the background noise. The

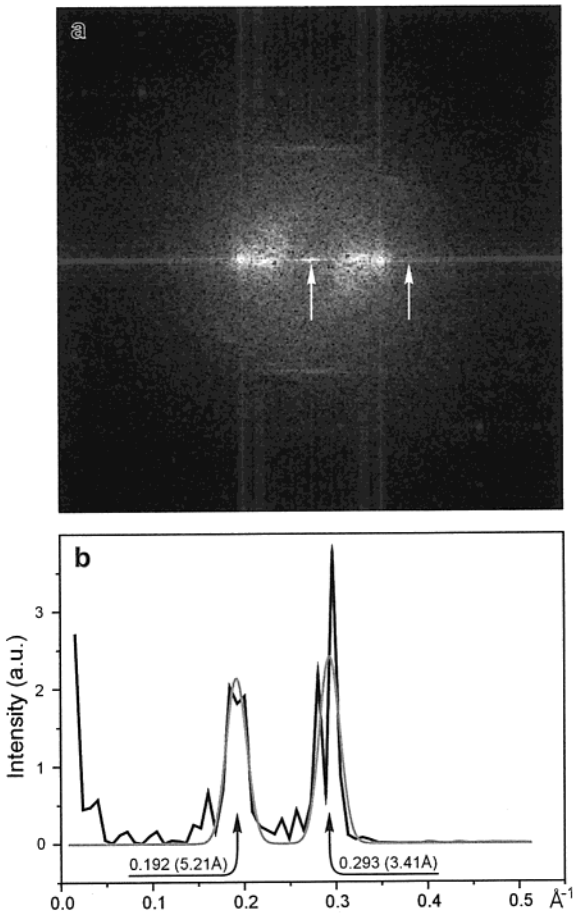

Figure 5. (a) FFT pattern of the TEM micrograph depicted in Figure 4. (b) Intensity profile of the pattern fitted with two Gaussian-shaped peaks.

part of the profile obtained on the inner section of the tube shows regular oscillations. The oscillation period is assumed to be 3.41 Å, which was derived from the position of the 002 reflection in the XRD pattern of the pristine carbon material. This value was taken as a reference standard to deduce the spacing of fluorine layers in the tube. The distance between dark fringes indicated by the arrows in the right of region 5 was estimated to be 5.21 Å.

Figure 4c−f shows the two-dimensional autocorrelation functions of the corresponding regions 1−4 of the image of the tube. The autocorrelation indicates a preferred orientation of layers along the tube surface even for the outer region 1, where the layers are significantly disordered. The curves at the left are profiles of the autocorrelations starting from the center in a direction perpendicular to the tube layers. The correlation peaks correspond to the average interlayer spacing. As is clearly seen, the layer separation increases from the inner part of the tube to its surface.

To estimate an average interlayer spacing for the fluorinated portion, a two-dimensional fast Fourier transform (FFT) of the micrograph from Figure 4a was carried out (Figure 5 a). An intensity profile of the FFT pattern along the 002 direction demonstrates two distinct sharp peaks (Figure 5b). These peaks were fitted by Gaussians positioned at 0.192 and 0.293 Å^{-1}. The more intense peak originates from the 002 spacing of the inner carbon shells and another peak corresponds

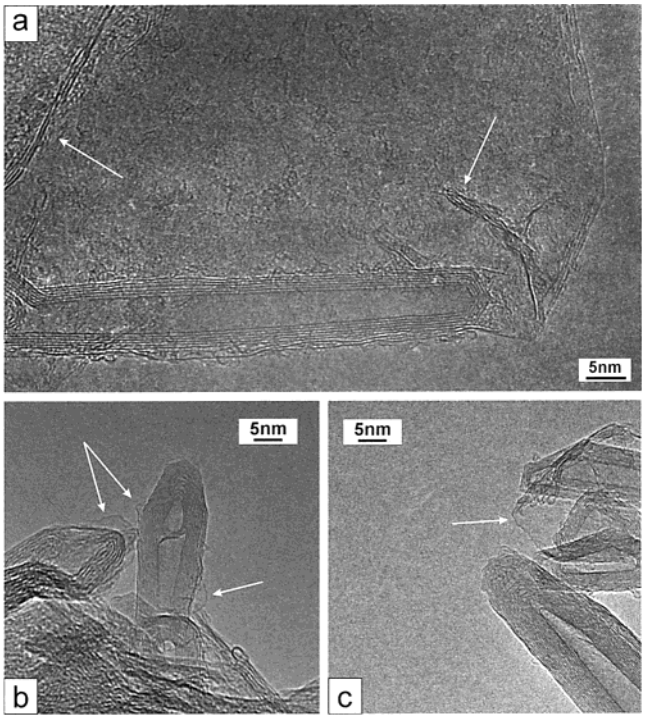

Figure 6. TEM micrographs of carbon nanotubes covered by thin fluorinated flakes (marked by arrows).

to an average interlayer spacing for the fluorinated part of the carbon nanotube of 5.21 Å, which confirms the findings of Figure 4. This value is considerably less than the interlayer spacing in C_2F of 6.02 Å. The diffraction from the fluorinated sections of the tube or polyhedral nanoparticles may appear as a shoulder at the high-angle side of the 002 reflection in the XRD pattern of the fluorinated carbon material (Figure 2c). In graphite fluoride the fluorine atoms are placed bilaterally along the carbon network. Because of the curvature of a graphite sheet rolled into a tube or polyhedral cage, its inner and outer surfaces would be distinct in chemical reactivity.[16] The predominant fluorination of the carbon nanotubes on one side of a shell and the low fluorine concentration between the layers might explain the lower interlayer spacing detected in the fluorinated nanotubes.

The carbon material contained various multilayer graphitic-like particles. The fluorination reduces an interlayer interaction leading, in some instances, to a separation of adjacent graphitic planes. HRTEM investigation of the produced sample (Figure 6) showed that the shells of carbon nanotubes might peel off. Figure 6a demonstrates a tube with walls that are different in a number of layers. Three additional layers of the bottom side of the tube represent the edge of a flake, as indicated by arrows. The monolayers on the carbon tube sides (Figure 6b) are most likely to be tube shells that have flaked off during fluorination. A three-layered flake in Figure 6c undoubtedly originates from the surface of the tubular particles because its edges reproduce contours of adjacent tubes. We believe the fluorinated flakes (Figure 6) came from the original nanotube walls, which were unrolled during the fluorination process. On the basis of these pictures and the observed fluorination process from the tube surface toward its cavity, a structure for these MWNTs may be suggested.

At the present time there are three structural models for arc-produced MWNTs:[17] (1) coaxial cylindrical shells (the "Russian doll" model); (2) the tube formed by a graphene sheet rolled into a scroll; 3) several inner shells that are cylindrical and the other layers scroll-shaped. In the case of the "Russian doll" model, molecules could penetrate between the shells only if the tube ends are open. However, the tubes formed in the cathode deposit are usually terminated by hemispheres or polyhedrons. The fluorination process of carbon nanotubes might be similar to that of graphite if a tube is composed of a multilayer scroll. Then, the reagents will penetrate into the intershell spacing of the nanotube by separating the layers of the scroll on its edge. As a result, the interaction of fluorinated layers with the nonfluorinated part of the tube is decreased, causing their peeling off, which would explain the occurrence of multisheet flakes in the product (Figures 1 and 6). The observation of nanotubes having about 10 fluorinated layers may be due to mechanical problems for unfolding the tube when it bundled to other particles (Figure 3c). The inner layers of the arc-produced carbon nanotubes are likely to be cylindrical, which would prevent their fluorination. Hence, we support the third model of the carbon nanotube, which combines scroll-like and concentric cylindrical shells.

4. Conclusion

Arc-produced carbon material consisting of multiwall tubes and polyhedral particles was fluorinated by a method that allows the production of graphite fluoride, C_2F. An IR and C 1s spectroscopy study indicated a similar characteristic of C−F bonding in the fluorinated sample and C_2F. The XRD patterns of the product exhibited the reflections characteristic of diffraction from both fluorinated graphitic layers and nonfluorinated ones. HRTEM images showed that only the outer shells of nanoparticles are fluorinated while the inner layers are well-graphitized. An observation of thin flakes adjacent to tubes suggests a partial or complete disruption of some nanotubes as a result of outer layers peeling off or the tube unfolding. We believe that most of the arc-produced carbon nanotubes are composed of nested scrolls while the inner shells, which remain nonfluorinated, are likely to be cylindrical. Application of intercalation procedures to the fluorinated material is expected to give additional information about the structure and formation process of MWNTs.

Acknowledgment. We would like to thank Dr. I. P. Asanov for the XPS measurements. This work was supported by INTAS (Projects Nos. 97-1700 and 00-237), the Russian Foundation for Basic Research (Grant 00-03-32510a), and the Russian scientific and technical program "Actual directions in physics of condensed states" on the "Fullerenes and atomic structures" (Project No. 98055) and the "Surface atomic structures" (Project No. 4.14.99).

CM0103141

(16) Blasé, X.; Benedict, L. X.; Shirley, E. L.; Louie, S. G. *Phys. Rev. Lett.* **1994**, *72*, 1878.

(17) Amelinckx, S.; Bernaerts, D.; Zhang, X. B.; Van Tendeloo, G.; Van Landuyt, J. *Science* **1995**, *267*, 1334.